

## 195. Radical Anions of Cyclic Azoalkanes: An ESR, ENDOR, and TRIPLE-Resonance Study

by Caspar H. Ess<sup>1)</sup> and Fabian Gerson\*

Institut für Physikalische Chemie der Universität Basel, Klingelbergstrasse 80, CH-4056 Basel

and Waldemar Adam

Institut für Organische Chemie der Universität Würzburg, Am Hubland, D-8700 Würzburg

(18.IX.91)

---

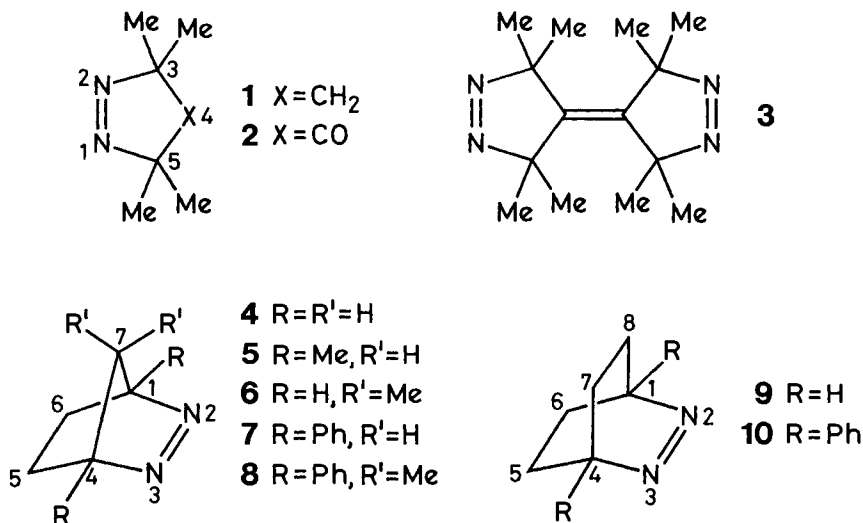
Radical anions of ten monocyclic and bicyclic azoalkanes containing the azo group in (*Z*)-conformation, have been fully characterized by their hyperfine data with the use of ESR, ENDOR, and general-TRIPLE-resonance spectroscopy. These azoalkanes are represented by 3,3,5,5-tetramethyl-1-pyrazoline (**1**), 2,3-diazabicyclo[2.2.1]hept-2-ene (**4**), and 2,3-diazabicyclo[2.2.2]oct-2-ene (**9**), as well as by their derivatives **2**, **3**, **5–8**, and **10**. For all radical anions **1**<sup>•–</sup>–**10**<sup>•–</sup>, the <sup>14</sup>N-coupling constant,  $a_N$ , is in the range of +0.83 to +0.97 mT; this finding indicates that the spin population is essentially restricted to the  $\pi$  system of the azo group. The <sup>14</sup>N-hyperfine anisotropy largely affects the width of ESR lines, particularly at low temperatures. Substantial coupling constants of <sup>7</sup>Li-, <sup>23</sup>Na-, <sup>39</sup>K-, and <sup>133</sup>Cs-nuclei point to a close association of the radical anions with their alkali-metal counterions. With the exception of <sup>39</sup>K, these nuclei give rise to readily observable ENDOR signals which appear along with those stemming from protons. The prominent hyperfine features of **1**<sup>•–</sup>–**10**<sup>•–</sup> are discussed.

---

**Introduction.** – Azoalkanes, in which the azo group is linked to saturated hydrocarbon moieties, have been known since 1909 [1]. Contrary to aromatic azo compounds like azobenzene, they readily lose N<sub>2</sub> upon a thermal or photolytical treatment [2], and this chemical property has been exploited to generate radicals, biradicals [2–4], and novel hydrocarbons [5]. Radical anions of several (*E*)-dialkyldiimines have been studied by ESR spectroscopy [6–8]. Persistent radical anions are, in general, produced from azoalkanes which, like di(*tert*-butyl)diimine, have no H-atoms in the positions neighbouring the azo group, or in which removal of these atoms is impeded by the *Bredt's* rule. Here, we report on such persistent radical anions generated from monocyclic and bicyclic azoalkanes containing the azo group in the (*Z*)-conformation. These compounds are represented by 3,3,5,5-tetramethyl-1-pyrazoline (**1**), 3,3,5,5-tetramethyl-1-pyrazol-4-one (**2**), 3,3,5,5,3',3',5',5'-octamethyldi(1-pyrazolinylidene) (**3**), 2,3-diazabicyclo[2.2.1]hept-2-ene (**4**) and its 1,4-dimethyl (**5**), 7,7-dimethyl (**6**), 1,4-diphenyl (**7**), and 1,4-diphenyl-7,7-dimethyl (**8**) derivatives and 2,3-diazabicyclo[2.2.2]oct-2-ene (**9**) and its 1,4-diphenyl (**10**) derivative. The radical anions **1**<sup>•–</sup>–**10**<sup>•–</sup> have been fully characterized by their hyperfine data with the use of ESR, ENDOR, and general-TRIPLE-resonance spectroscopy.

---

<sup>1)</sup> Present address: Department of Chemistry, Stanford University, California 94305, U.S.A.



**Results and Discussion.** – *Generation and Stability of the Radical Anions.* Due to the presence of the electron-attracting azo group, the compounds **1–10** were easily reduced to their radical anions. Cyclic voltammograms of **1**, **4**, and **9** (solvent: CH<sub>3</sub>CN; working electrode: Hg; counter-electrode: Ag/AgCl; supporting salt: Bu<sub>4</sub>NClO<sub>4</sub>; scan: 200mV/s; temperature: 298 K) exhibited reversible waves at half-wave potentials,  $E_{1/2}$  (vs. SCE), of  $-0.82 \pm 0.01$ ,  $-0.87 \pm 0.01$ , and  $-0.82 \pm 0.01$  V, respectively. For spectroscopic studies, the radical anions **1"–10"** were prepared from the corresponding neutral compounds by reaction with an alkali-metal mirror in 1,2-dimethoxyethane (DME). Direct use of the metallic K, Na, or Cs led to the radical anions associated with K<sup>+</sup>, Na<sup>+</sup>, or Cs<sup>+</sup>, while adding an excess of LiCl salt to the solution of a radical anion, produced by reduction with K, caused replacement of K<sup>+</sup> by Li<sup>+</sup> as the counterion.

As indicated by their moderately negative potentials  $E_{1/2}$  and by reversibility of their reduction waves in the cyclic voltammograms, the radical anions **1"–10"** were thermodynamically and kinetically stable. The kinetic stability (persistence) of **1"–10"** is not unexpected, considering their molecular structures which meet the requirements stated in the *Introduction*. In the diazabicycloalkene series, the persistence of the radical anions was lowered by dimethyl or diphenyl substitution at the bridgehead atoms C(1) and C(4), presumably because such a substitution promotes exclusion of N<sub>2</sub> by stabilizing thus formed radicals or biradicals [9]. Therefore, **5"** and **7"** were less persistent than **4"**, and the persistence of **10"** was lower than that of **9"**. By contrast, dimethyl substitution at the methano-bridge atom C(7) of diazabicycloheptene seemed to enhance the persistence of the radical anions, **8"** being as stable as **4"** despite the presence of Ph groups at C(1) and C(4).

*ESR Spectra.* The radical anions **1"–10"** were studied by ESR spectroscopy from 203 K up to the temperature at which their decay set in. The resolution of the spectra was strongly affected by <sup>14</sup>N-hyperfine anisotropy, especially at low temperatures. In

consequence, the line-widths increased on going from the centres of the spectra to the peripheries and, to a lesser extent, on passing from the low- to the high-field halves (see *Appendix*). Temperature-dependent hyperfine splittings from alkali-metal nuclei of the counterions were observed for all radical anions. The pertinent nuclei are  ${}^7\text{Li}$ ,  ${}^{23}\text{Na}$ ,  ${}^{39}\text{K}$ , or  ${}^{133}\text{Cs}$  for **1**<sup>-</sup>–**3**<sup>-</sup> associated with  $\text{Li}^+$ ,  $\text{Na}^+$ ,  $\text{K}^+$ , or  $\text{Cs}^+$ , and they are  ${}^7\text{Li}$ ,  ${}^{39}\text{K}$ , or  ${}^{133}\text{Cs}$  for **4**<sup>-</sup>–**10**<sup>-</sup> with  $\text{Li}^+$ ,  $\text{K}^+$ , or  $\text{Cs}^+$  as the counterions. In the latter case,  ${}^{23}\text{Na}$ -hyperfine splittings could not be determined. Brief contact of the solutions of **4**–**10** with Na mirror in DME gave rise to low-intensity spectra identical to those observed with the counterion  $\text{K}^+$  (see *Experimental*), while upon prolonged reduction these spectra were superseded by an unresolved S-shaped derivative curve. Interestingly, the  ${}^7\text{Li}$ -hyperfine splittings indicated association of **1**<sup>-</sup>–**10**<sup>-</sup> with two  $\text{Li}^+$  counterions, presumably due to the addition of  $\text{LiCl}$  salt in a concentration largely exceeding that of the radical anion.

It is noteworthy that the ESR spectra of **3**<sup>-</sup> were very similar to those of **1**<sup>-</sup> and **2**<sup>-</sup> under the applied experimental conditions (solvent: DME; counterion:  $\text{Li}^+$ ,  $\text{Na}^+$ ,  $\text{K}^+$ , or  $\text{Cs}^+$ ; temperature: 203–293 K). Thus, under these conditions, the unpaired electron in **3**<sup>-</sup> appears to be localized on one 1-pyrazoline moiety, *i.e.*, electron-spin transfer between the two moieties is slow on the hyperfine time-scale ( $\sim 10^7 \text{ s}^{-1}$ ).

The ESR spectra, taken at 203 K are exemplified in *Figs. 1* and *2* by those of **1**<sup>-</sup> associated with  $\text{Li}^+$ ,  $\text{Na}^+$ ,  $\text{K}^+$ , or  $\text{Cs}^+$ , and of **4**<sup>-</sup> with  $\text{Li}^+$ ,  $\text{K}^+$ , or  $\text{Cs}^+$  as the counterions. Their temperature dependence is illustrated in *Fig. 3* by the spectra of **1**<sup>-</sup>/ $\text{K}^+$  at 203 and 273 K. Analyses of all spectra were supported by computer simulations, as demonstrated in *Fig. 4* for **1**<sup>-</sup>/ $\text{Na}^+$  at 273 K, and by the use of the ENDOR technique.

*ENDOR Spectra.* All radical anions **1**<sup>-</sup>–**10**<sup>-</sup> gave rise, at 203 K, to  ${}^1\text{H}$ -ENDOR spectra, except for **4**<sup>-</sup>–**10**<sup>-</sup> associated with  $\text{Na}^+$ ; in this case, the unresolved S-shaped ESR absorption did not respond to the ENDOR experiment. The signals appeared pairwise at  $\nu_{\text{H}} \pm \frac{1}{2}|a_{\text{H}}|$  where  $\nu_{\text{H}} = 14.56 \text{ MHz}$  is the frequency of the free proton, and  $a_{\text{H}}$  represents the  ${}^1\text{H}$ -coupling constant in MHz [10a]. In addition, ENDOR signals from  ${}^7\text{Li}$ -,  ${}^{23}\text{Na}$ -, or  ${}^{133}\text{Cs}$ -nuclei were detected for **1**<sup>-</sup>–**3**<sup>-</sup> associated with  $\text{Li}^+$ ,  $\text{Na}^+$ , or  $\text{Cs}^+$ , and for **4**<sup>-</sup>–**10**<sup>-</sup> with  $\text{Li}^+$  or  $\text{Cs}^+$  as the counterions. Whereas in the case of  ${}^7\text{Li}$  and  ${}^{133}\text{Cs}$  high- as well as low-frequency signals could be observed at  $\nu_{\text{Li}} \pm \frac{1}{2}|a_{\text{Li}}|$  or  $\frac{1}{2}|a_{\text{Cs}}| \pm \nu_{\text{Cs}}$ , only the high-frequency signal at  $\nu_{\text{Na}} + \frac{1}{2}|a_{\text{Na}}|$  was detected for  ${}^{23}\text{Na}$ , because of the low sensitivity of our ENDOR system in the range of 0–3 MHz pertinent to  $\nu_{\text{Na}} - \frac{1}{2}|a_{\text{Na}}|$ . For the same reason, both  ${}^{39}\text{K}$ -ENDOR signals escaped detection ( $|a_{\text{K}}| \approx 1.4 \text{ MHz}$  or  $0.05 \text{ mT}$  in the ESR spectra;  $\frac{1}{2}|a_{\text{K}}| - \nu_{\text{K}} \approx 0$ ;  $\frac{1}{2}|a_{\text{K}}| + \nu_{\text{K}} \approx 1.4 \text{ MHz}$ ). Here,  $\nu_{\text{Li}} = 5.66$ ,  $\nu_{\text{Na}} = 3.85$ ,  $\nu_{\text{K}} = 0.68$ , and  $\nu_{\text{Cs}} = 1.91 \text{ MHz}$  are the free frequencies of the  ${}^7\text{Li}$ -,  ${}^{23}\text{Na}$ -,  ${}^{39}\text{K}$ -, and  ${}^{133}\text{Cs}$ -nuclei, while  $a_{\text{Li}}$ ,  $a_{\text{Na}}$ ,  $a_{\text{K}}$ , and  $a_{\text{Cs}}$  represent the corresponding alkali-metal-coupling constants in MHz [10b]. The  ${}^{14}\text{N}$ -ENDOR signals failed to appear in the range of 10.5–15 MHz, expected for  $\frac{1}{2}|a_{\text{N}}| \pm \nu_{\text{N}}$ , considering the frequency  $\nu_{\text{N}} = 1.05 \text{ MHz}$  of the free nucleus and the coupling constant  $|a_{\text{N}}| = 23$ – $28 \text{ MHz}$  (which corresponds to  $|a_{\text{N}}| = 0.83$  to  $0.97 \text{ mT}$  in the ESR spectra). In this case, the  ${}^{14}\text{N}$ -hyperfine enhancement factor [10b] was insufficient to allow observation by the ENDOR technique. *Figs. 5* and *6* reproduce the  ${}^1\text{H}$ - and alkali-metal-ENDOR spectra of **1**<sup>-</sup> associated with  $\text{Li}^+$ ,  $\text{Na}^+$ , or  $\text{Cs}^+$  and of **4**<sup>-</sup> with  $\text{Li}^+$  or  $\text{Cs}^+$  as the counterions. These spectra were taken under the same conditions as their ESR counterparts in *Figs. 1* and *2*.

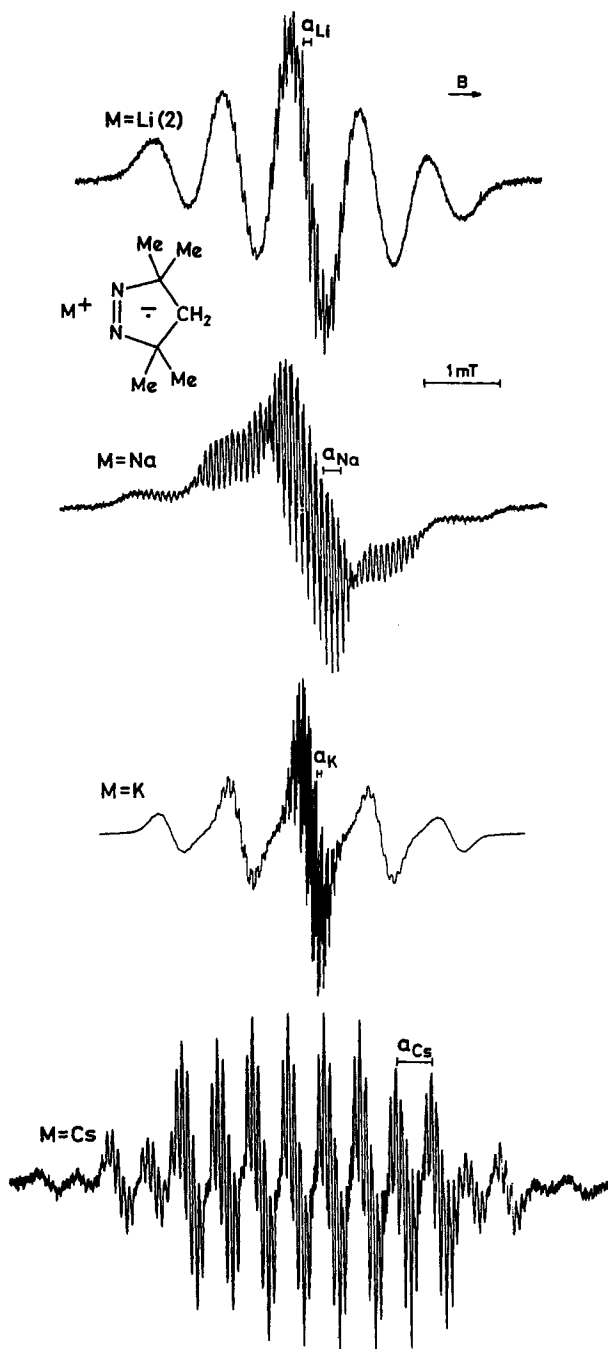


Fig. 1. ESR spectra of  $1^{\bullet-}$ . Solvent: DME; counterion as indicated; temp.: 203 K.  $M = \text{Li}(2)$  signifies that two  $\text{Li}^+$  counterions are associated with each radical anion.

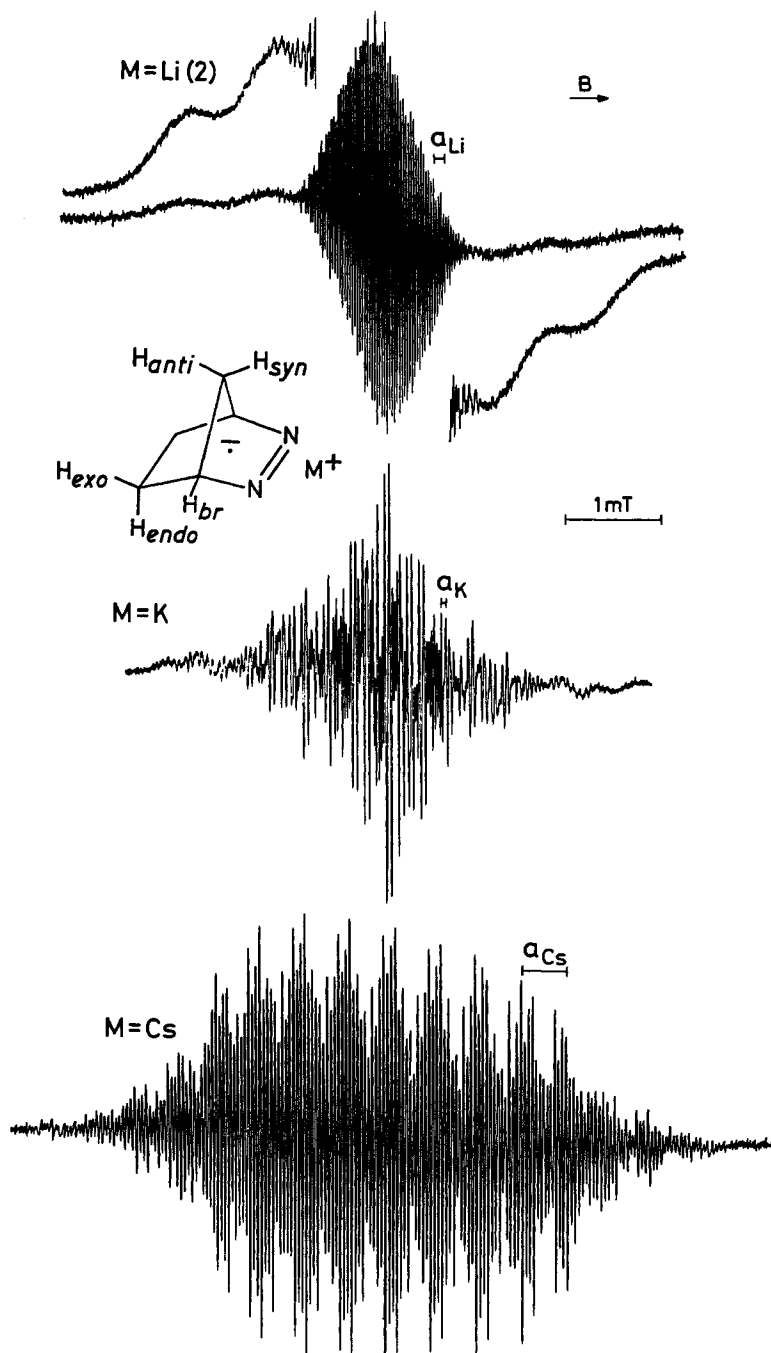


Fig. 2. ESR spectra of  $4^{\bullet-}$ . Solvent: DME; counterion as indicated; temp.: 203 K. The insets in the uppermost spectrum were recorded using higher modulation.  $M = \text{Li}(2)$  signifies that two  $\text{Li}^+$  counterions are associated with each radical anion.

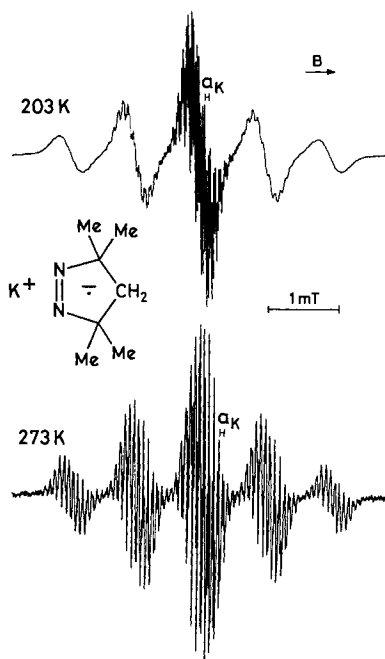


Fig. 3. ESR spectra of **1**<sup>•</sup>. Solvent: DME; counterion and temp. as indicated.

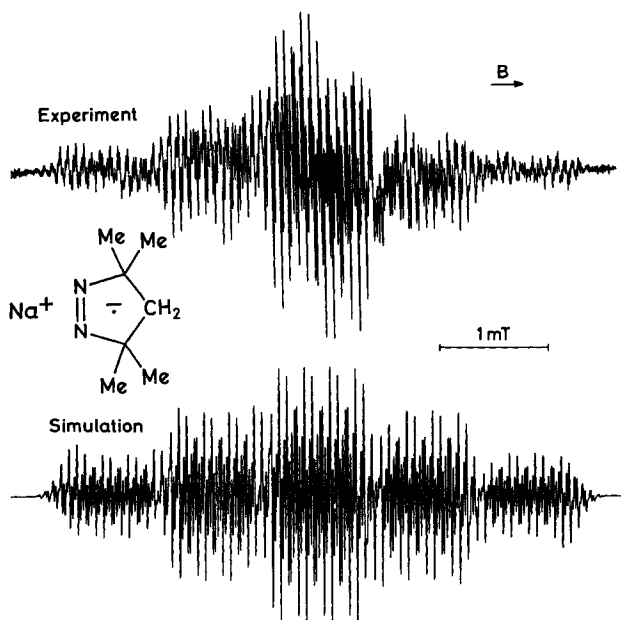


Fig. 4. ESR spectrum of **1**<sup>•</sup> and its simulation. Solvent: DME; counterion as indicated; temp.: 273 K. The simulation makes use of the coupling constants given in Table I; line-shape: Lorentzian; line-width (constant): 0.024 mT, without accounting for the effects of <sup>14</sup>N-hyperfine anisotropy (see Appendix).

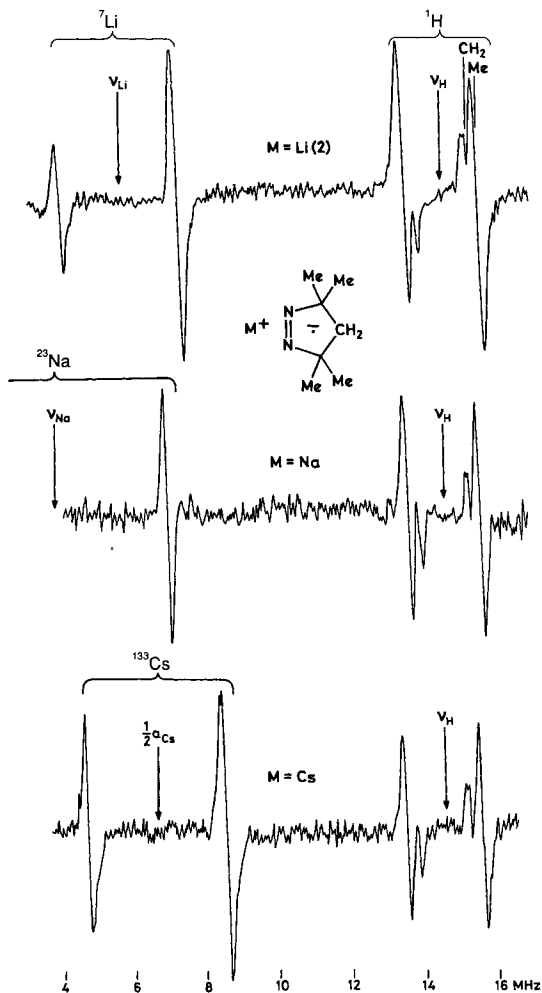


Fig. 5.  $^1\text{H}$ -,  $^7\text{Li}$ -,  $^{23}\text{Na}$ -, and  $^{133}\text{Cs}$ -ENDOR spectra of  $\mathbf{1}^-$ . Experimental conditions as for Fig. 1.

*Signs and Assignments of the Coupling Constants.* The hyperfine data for all radical anions  $\mathbf{1}^-$ – $\mathbf{10}^-$  and their counterions are listed in Tables 1, 2, and 3 (for  $\mathbf{9}^-$ , see also [11]), together with the corresponding  $g$  factors. The signs allotted to the coupling constants have been derived by a general-TRIPLE-resonance experiment [10a] combined with theoretical arguments. The TRIPLE-resonance technique yielded relative signs of the coupling constants for all nuclei which gave rise to pairs of ENDOR signals, *i.e.*, for  $^1\text{H}$ ,  $^7\text{Li}$ , and  $^{133}\text{Cs}$ . In the case of  $\mathbf{4}^-$ – $\mathbf{10}^-$  (Tables 2 and 3), the absolute signs were obtained on the reasonable assumption that the largest values  $|a_{\text{H}}|$  due to the protons in the *exo*-positions of the ethano bridges (see below) are positive. As the signs of  $a_{\text{Li}}$  and  $a_{\text{Cs}}$  for the counterions  $\text{Li}^+$  or  $\text{Cs}^+$  associated with  $\mathbf{4}^-$ – $\mathbf{10}^-$  are opposite and equal, respectively, to that of  $a_{\text{Hexo}}$ , a negative sign is indicated for  $a_{\text{Li}}$  and a positive one for  $a_{\text{Cs}}$ . These signs must also be shared by  $^7\text{Li}$ - and

$^{133}\text{Cs}$ -coupling constants for **1**–**3** with  $\text{Li}^+$  or  $\text{Cs}^+$  as the counterions, because *i*) here, too, general-TRIPLE-resonance experiments required opposite signs of  $a_{\text{Li}}$  and  $a_{\text{Cs}}$  and *ii*) the values of  $|a_{\text{Li}}|$  as well as those of  $|a_{\text{Cs}}|$  were very similar in the two series, thus pointing to a closely related mode of association of the radical anions with the same counterions. In turn, using  $a_{\text{Li}}$  and  $a_{\text{Cs}}$  as reference, absolute signs could be allotted to the coupling constants  $a_{\text{H}}(\text{CH}_2)$  for **1** and  $a_{\text{H}}(\text{Me})$  for **1**–**3** with the use of general-TRIPLE-resonance spectroscopy (Table 1).

The signs of  $a_{\text{Na}}$  (absence of the low-frequency  $^{23}\text{Na}$ -signals) and  $a_{\text{K}}$  (failure to detect both  $^{39}\text{K}$ -signals) could not be determined in this way. However, the temperature dependence of  $a_{\text{Na}}$  and  $a_{\text{K}}$  indicated that the two coupling constants have the same positive sign as  $a_{\text{Cs}}$  which is opposite to that of  $a_{\text{Li}}$  (see below). The sign of the large  $^{14}\text{N}$ -coupling constant,  $a_{\text{N}}$ , is also certainly positive, as it is in other radical ions in which the N-atoms bear a substantial part of the spin population. This sign is consistent with the ESR lines being broader in the high- than in the low-field half of the spectrum [12a][13].

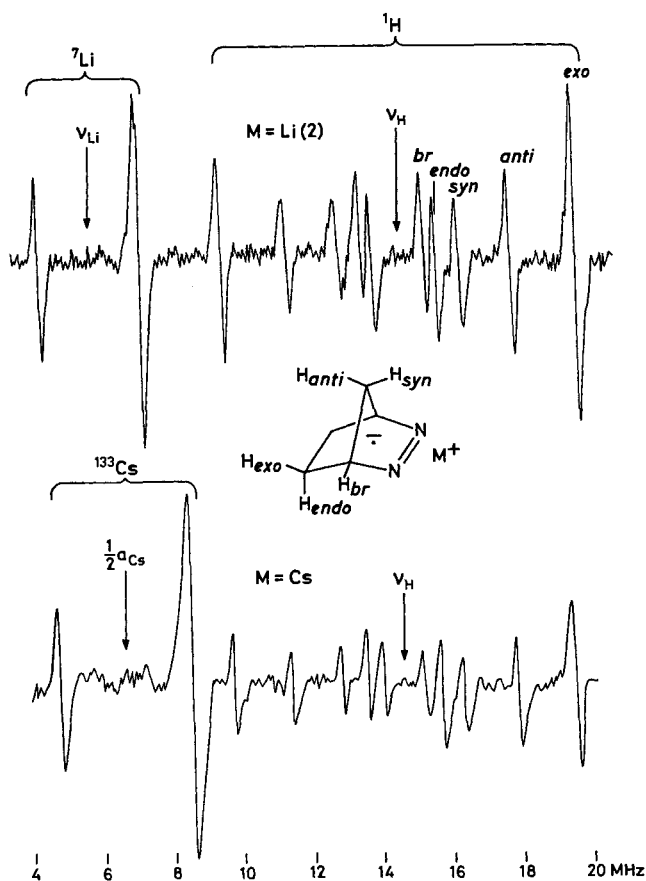


Fig. 6.  $^1\text{H}$ -,  $^7\text{Li}$ -, and  $^{133}\text{Cs}$ -ENDOR spectra of **4**. Experimental conditions as for Fig. 2.



Assignments of the coupling constants to sets of equivalent nuclei other than protons are unproblematic, due to their specific quantum numbers  $I$ , strongly differing values, and characteristic frequencies of the free nuclei in the ENDOR spectra. As for the coupling constants  $a_H$ , assignments are also in most cases straightforward, owing to different multiplicities of the sets of equivalent protons and to effects of dimethyl or diphenyl substitution. The only protons which cannot be distinguished by experimental evidence are those in the *syn*- and *anti*-positions at C(7) for **4**" , **5**" , and **7**" (or in the corresponding Me substituents for **6**" and **8**" ) and in the *exo*- and *endo*-positions at C(5) and C(6) for **4**"–**8**" or at C(5), C(6), C(7), and C(8) for **9**" and **10**" . In these cases, assignments of coupling constants to protons in the individual positions have been guided by analogy with structurally related radical ions (see, e.g., [14][15]) for which always  $|a_{H_{anti}}| > |a_{H_{syn}}|$  and  $|a_{H_{exo}}| > |a_{H_{endo}}|$ . These assignments are supported by theory, as shown in Table 4 by comparison of the  $^1\text{H}$ - and  $^{14}\text{N}$ -coupling constants, observed for **4**" and **9**" with the corresponding values calculated by the INDO procedure [16] and based on an MNDO-optimized geometry [17]. There is a fair agreement between experiment and theory, except for the sign of  $a_{H_{endo}}$ .

Table 1. Coupling Constants [mT] and  $g$  Factors for **1**"–**3**". Solvent: DME.

<b>1</b> "									
Counterion, M <sup>+</sup>	Li <sup>+</sup> b)		Na <sup>+</sup>		K <sup>+</sup>		Cs <sup>+</sup>		
	Temp.[K]	203	293	203	273	203	273	203	
$a_H$ (CH <sub>2</sub> , 2 H)	+0.049		<sup>c)</sup>	+0.051	+0.050	+0.048	+0.048	+0.052	+0.049
$a_H$ (Me, 12 H)	-0.071		<sup>c)</sup>	-0.072	-0.071	-0.074	-0.072	-0.074	-0.071
$a_N$ (2 N)	+0.888	+0.890		+0.931	+0.933	+0.918	+0.923	+0.930	+0.932
$a_M$	-0.116		<sup>c)</sup>	+0.224	+0.236	+0.048	+0.058	+0.472	+0.554
$g$ factor	2.0037			2.0037		2.0037		2.0041	
<b>2</b> "									
Counterion, M <sup>+</sup>	Li <sup>+</sup> b)		Na <sup>+</sup>		K <sup>+</sup>		Cs <sup>+</sup>		
	Temp.[K]	203	273	203	253	203	253	203	
$a_H$ (Me, 12 H)	-0.061	-0.060		-0.063	-0.059	-0.062	-0.060	-0.061	-0.061
$a_N$ (2 N)	+0.892	+0.902		+0.938	+0.945	+0.927	+0.938	+0.918	+0.940
$a_M$	-0.117	-0.097		+0.206	+0.218	+0.047	+0.052	+0.420	+0.470
$g$ factor	2.0038			2.0039		2.0039		2.0042	
<b>3</b> "									
Counterion, M <sup>+</sup>	Li <sup>+</sup> b)		Na <sup>+</sup>		K <sup>+</sup>		Cs <sup>+</sup>		
	Temp.[K]	203	293	203	293	203	273	203	
$a_H$ (Me, 12 H)	-0.089	-0.085		-0.094	-0.089	-0.091	-0.088	-0.092	-0.085
$a_N$ (2 N)	+0.872	+0.874		+0.908	+0.910	+0.896	+0.898	+0.888	+0.902
$a_M$	-0.119	-0.099		+0.208	+0.216	+0.048	+0.053	+0.448	+0.527
$g$ factor	2.0036			2.0036		2.0037		2.0042	

a) Experimental error:  $\pm 0.001$  mT in  $a_H$  and  $a_M$ ,  $\pm 0.005$  mT in  $a_N$  at 203 K,  $\pm 0.005$  mT in  $a_H$ ,  $a_M$ , and  $a_N$  at higher temperatures,  $\pm 0.0001$  in  $g$ .

b) Two Li<sup>+</sup> counterions per radical anion.

c) Not determined.

Table 2. Coupling Constants [mT] and g Factors for 4<sup>u</sup>-8<sup>h</sup>). Solvent: DME.

4 <sup>u</sup>						
Counterion, M <sup>+</sup>	Li <sup>+</sup> b)		K <sup>+</sup>		Cs <sup>+</sup>	
	Temp. [K]					
a <sub>Hexo</sub> (2 H)	203	293	203	293	203	293
a <sub>Hexo</sub> (2 H)	+0.362	+0.358	+0.355	+0.340	+0.348	+0.337
a <sub>Endo</sub> (2 H)	-0.076	-0.075	-0.076	-0.073	-0.075	-0.074
a <sub>Hanti</sub> (1 H)	-0.228	-0.225	-0.232	-0.223	-0.229	-0.221
a <sub>Hsyn</sub> (1 H)	-0.122	-0.113	-0.127	-0.122	-0.123	-0.116
a <sub>Hbr</sub> (2 H)	+0.054	+0.053	+0.046	+0.044	+0.041	+0.039
a <sub>N</sub> (2 N)	+0.848	+0.846	+0.871	+0.855	+0.856	+0.834
a <sub>M</sub>	-0.104	-0.053	+0.053	+0.055	+0.469	+0.493
g factor	2.0038		2.0039		2.0042	
5 <sup>u</sup>						
Counterion, M <sup>+</sup>	Li <sup>+</sup> b)		K <sup>+</sup>		Cs <sup>+</sup>	
	Temp. [K]					
a <sub>Hexo</sub> (2 H)	203	c)	203	c)	203	c)
a <sub>Hexo</sub> (2 H)	+0.432		+0.422		+0.418	
a <sub>Endo</sub> (2 H)	-0.057		-0.057		-0.058	
a <sub>Hanti</sub> (1 H)	-0.212		-0.215		0.213	
a <sub>Hsyn</sub> (1 H)	-0.114		-0.115		-0.116	
a <sub>Hbr</sub> (Me, 6 H)	-0.028		-0.027		-0.026	
a <sub>N</sub> (2 N)	+0.843		+0.852		+0.868	
a <sub>M</sub>	-0.107		+0.050		+0.450	
g factor	2.0038		2.0039		2.0041	
6 <sup>u</sup>						
Counterion, M <sup>+</sup>	Li <sup>+</sup> b)		K <sup>+</sup>		Cs <sup>+</sup>	
	Temp. [K]					
a <sub>Hexo</sub> (2 H)	203	293	203	293	203	293
a <sub>Hexo</sub> (2 H)	+0.421	+0.415	+0.409	+0.406	+0.406	+0.400
a <sub>Endo</sub> (2 H)	-0.067	-0.067	-0.064	-0.065	-0.059	-0.059
a <sub>Hanti</sub> (Me, 3 H)	+0.133	+0.136	+0.136	+0.139	+0.139	+0.139
a <sub>Hsyn</sub> (Me, 3 H)	+0.013	+0.013	+0.010	+0.012	+0.012	+0.010
a <sub>Hbr</sub> (2 H)	<0.010	<0.010	<0.010	<0.010	<0.010	<0.010
a <sub>N</sub> (2 N)	+0.880	+0.872	+0.852	+0.848	+0.864	+0.853
a <sub>M</sub>	-0.102	-0.055	+0.050	+0.058	+0.482	+0.546
g factor	2.0038		2.0039		2.0042	
7 <sup>u</sup>						
Counterion, M <sup>+</sup>	Li <sup>+</sup> b)		K <sup>+</sup>		Cs <sup>+</sup>	
	Temp. [K]					
a <sub>Hexo</sub> (2 H)	203	c)	203	c)	203	c)
a <sub>Hexo</sub> (2 H)	+0.435		+0.434		+0.432	
a <sub>Endo</sub> (2 H)	-0.065		-0.062		-0.062	
a <sub>Hanti</sub> (1 H)	-0.211		-0.216		-0.213	
a <sub>Hsyn</sub> (1 H)	-0.115		-0.118		-0.117	
a <sub>Hbr</sub> (Ph, 10 H)	<0.005		<0.005		<0.005	
a <sub>N</sub> (2 N)	+0.848		+0.848		+0.867	
a <sub>M</sub>	-0.103		+0.046		+0.433	
g factor	2.0038		2.0038		2.0042	

Table 2 (cont.)

8 <sup>a</sup>						
Counterion, M <sup>+</sup>	Li <sup>+</sup> b)		K <sup>+</sup>		Cs <sup>+</sup>	
	Temp. [K]	203	293	203	293	203
a <sub>Hexo</sub> (2 H)	+0.514	+0.505	+0.484	+0.482	+0.485	+0.484
a <sub>Hendo</sub> (2 H)	-0.043	-0.043	-0.044	-0.042	-0.044	-0.045
a <sub>Hanti</sub> (Me, 3 H)	+0.111	+0.113	+0.127	+0.121	+0.126	+0.131
a <sub>Hsyn</sub> (Me, 3 H)	<0.010	<0.010	<0.010	<0.010	<0.010	<0.010
a <sub>Hbr</sub> (Ph, 10 H)	<0.010	<0.010	<0.010	<0.010	<0.010	<0.010
a <sub>N</sub> (2 N)	+0.858	+0.840	+0.888	+0.844	+0.972	+0.898
a <sub>M</sub>	-0.099	-0.038	+0.049	+0.052	+0.488	+0.529
g factor	2.0038		2.0038		2.0042	

a) Experimental error:  $\pm 0.001$  mT in a<sub>H</sub> and a<sub>M</sub>,  $\pm 0.005$  mT in a<sub>N</sub> at 203 K,  $\pm 0.005$  mT in a<sub>H</sub>, a<sub>M</sub>, and a<sub>N</sub> at higher temperatures,  $\pm 0.0001$  in g.

b) Two Li<sup>+</sup> counterions per radical anion.

c) Unstable at higher temperatures.

Table 3. Coupling Constants [mT] and g Factors for 9<sup>a</sup> and 10<sup>a</sup>). Solvent: DME.

9 <sup>a</sup>						
Counterion, M <sup>+</sup>	Li <sup>+</sup> b)		K <sup>+</sup>		Cs <sup>+</sup>	
	Temp. [K]	203	293	203 <sup>c)</sup>	293	203
a <sub>Hexo</sub> (4 H)	+0.276	+0.272	+0.274	+0.268	+0.274	+0.272
a <sub>Hendo</sub> (4 H)	-0.073	-0.077	-0.073	-0.071	-0.073	-0.067
a <sub>Hbr</sub> (2 H)	-0.019	-0.020	-0.020	-0.020	-0.020	-0.018
a <sub>N</sub> (2 N)	+0.858	+0.852	+0.878	+0.876	+0.880	+0.883
a <sub>M</sub>	-0.112	<0.015	+0.053	+0.061	+0.481	+0.547
g factor	2.0039		2.0040		2.0042	

10 <sup>a</sup>						
Counterion, M <sup>+</sup>	Li <sup>+</sup> b)		K <sup>+</sup>		Cs <sup>+</sup>	
	Temp. [K]	203	293	203	<sup>d)</sup>	203
a <sub>Hexo</sub> (4 H)	+0.289	+0.287	+0.301		+0.304	
a <sub>Hendo</sub> (4 H)	-0.066	-0.065	-0.065		-0.062	
a <sub>Hbr</sub> (Ph, 10 H)	<0.010	<0.015	<0.010		<0.010	
a <sub>N</sub> (2 N)	+0.862	+0.858	+0.867		+0.870	
a <sub>M</sub>	-0.066	<0.015	+0.048		+0.435	
g factor	2.0039		2.0039		2.0041	

a) Experimental error:  $\pm 0.001$  mT in a<sub>H</sub> and a<sub>M</sub>,  $\pm 0.005$  mT in a<sub>N</sub> at 203 K,  $\pm 0.005$  mT in a<sub>H</sub>, a<sub>M</sub>, and a<sub>N</sub> at higher temperatures,  $\pm 0.0001$  in g.

b) Two Li<sup>+</sup> counterions per radical anion.

c) The values given in this column were quoted in [11].

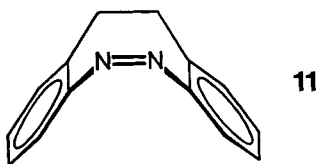
d) Unstable at higher temperatures.

Table 4. Comparison of Observed and Calculated Coupling Constants [mT] for **4''** and **9''**.

	<b>4''</b>		<b>9''</b>	
	Calc. <sup>a)</sup>	Obs. <sup>b)</sup>	Calc. <sup>a)</sup>	Obs. <sup>b)</sup>
$a_{\text{Hexo}}$	+0.278	+0.355	+0.223	+0.274
$a_{\text{Hendo}}$	+0.066	-0.076	+0.037	-0.073
$a_{\text{Hanti}}$	-0.216	-0.232	–	–
$a_{\text{Hsyn}}$	-0.082	-0.127	–	–
$a_{\text{Hbr}}$	+0.019	+0.046	-0.047	-0.020
$a_{\text{N}}$	+0.621	+0.871	+0.671	+0.878

<sup>a)</sup> See text for the procedure.  
<sup>b)</sup> Solvent: DME; counterion: K<sup>+</sup>; temp.: 203 K.

<sup>14</sup>N- and <sup>1</sup>H-Coupling Constants: Spin Distribution. The singly occupied orbital in the radical anions of azo compounds is essentially an antibonding  $\pi$  MO of the –N=N– group. In the azoarenes, there is a substantial conjugation between the  $\pi$  system of this group and those of the aromatic moieties. The <sup>14</sup>N-coupling constant,  $a_{\text{N}}$ , for the radical anion of (*E*)-azobenzene is +0.45 to 0.50 mT (dependent on the experimental conditions [18]) and it is *ca.* +0.40 mT for the radical anions of (*E*)-azonaphthalenes [19]. In these species, the two N-atoms of the azo group accommodate *ca.* 40–45% of the  $\pi$ -spin population. On passing to the radical anions of azoalkanes, the  $a_{\text{N}}$  value nearly doubles; irrespective of the conformation of the azo group and the structure of the alkane moieties, it is +0.78 to +0.97 mT, ([6–8], Tables 1–3). The  $\pi$ -spin population in the radical anions of azoalkanes is thus, to the extent of 80–90%, restricted to the azo group. An impressive example is provided by the radical anion of 5,6-dihydrodibenzo[*c,g*][1,2]diazocine (**11**)



which is a bridged derivative of (*Z*)-azobenzene. The  $a_{\text{N}}$  value for **11** is +0.915 mT [19], *i.e.*, it resembles that for the radical anions of azoalkanes, because the non-planar geometry of **11** impairs an effective conjugation between the azo group and the aromatic moieties. Correspondingly, the coupling constants of the protons of these moieties are very strongly reduced relative to corresponding values for the radical anion of (*E*)-azobenzene.

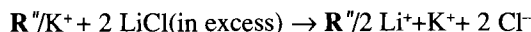
According to ESR nomenclature [12b], bridgehead protons ( $H_{\text{br}}$ ) which are separated from the  $\pi$  system of the azo group in **4''**, **6''**, and **9''**, have to be denoted  $\beta$ , while the methano *syn*- and *anti*-protons ( $H_{\text{syn}}$  and  $H_{\text{anti}}$ ) in **4''**, **5''** and **7''**, as well as the ethano *endo*-

and *exo*-protons ( $H_{endo}$  and  $H_{exo}$ ) in **4**"–**10**", should be called  $\gamma$ . The hyperfine interaction of the  $\beta$ -protons with the unpaired electron in a  $\pi$  system mainly implies hyperconjugation and is, thus, proportional to  $\cos^2\theta$  where  $\theta$  represents the dihedral angle between the  $p_z$ -axis at the adjacent  $\pi$  centre and the direction of the C– $H_\beta$  bond [20]. As the sign of the coupling constant  $a_{H\beta}$  is the same as that of the  $\pi$ -spin population at this centre, it is usually positive. The small  $a_{H\beta}$  value (+0.05 mT) for **4**" complies with the large angle  $\theta$  (ca. 75°) in diazabicycloheptenes. Enlargement of the C-framework to that of diazabicyclooctene increases  $\theta$  to 90°, *i.e.*, the bridgehead protons come to lie in plane of the  $\pi$  system of the azo group. Hyperconjugation is, thus, ineffective in **9**", and only spin polarization contributes to  $a_{H\beta}$ , resulting in a very small and negative value (–0.02 mT). Although coupling to the  $\gamma$ -protons is, in general, considerably weaker than to the  $\beta$ -protons [12b], special arrangements of the C– $H_\gamma$  bonds relative to the  $p_z$ -axis at a  $\pi$  centre can greatly favour the  $\gamma$ -proton-hyperfine interaction with the unpaired electron. This is the case for  $H_{exo}$  in **4**"–**10**" and, to a lesser extent, for  $H_{anti}$  in **4**", **5**", and **7**", such an arrangement occurring in a W or zig-zag fashion [14]. A long-range electron transfer of this kind is referred to as homohyperconjugation or through-bond interaction [21]. The values of  $a_{H_{exo}}$  are relatively large and positive (+0.34 to +0.51 mT for **4**"–**8**" and +0.27 to +0.30 mT for **9**" and **10**"), whereas those of  $a_{H_{anti}}$  are smaller in magnitude and negative (–0.21 to –0.23 mT). This sign of  $a_{H_{anti}}$  must be due to the location of the  $CH_2$  bridge in the nodal plane of the singly occupied, antibonding MO of the azo group. Substitution of  $H_{anti}$  at C(7) by a Me group, on going from **4**" to **6**" and from **7**" to **8**", replaces the coupling constant of a  $\gamma$ -proton by that of three  $\delta$ -protons which are separated from the  $\pi$  system by an additional  $sp^3$ -hybridized atom. Interestingly, the coupling constant of these  $\delta$ -protons still retains half of the  $|a_{H_{anti}}|$  value, but its sign changes to positive (+0.11 to +0.13 mT). Molecular models indicate that the C– $H_\delta$  bonds in several conformations of the Me group adopt the favourable zig-zag arrangement relative to the  $p_z$ -axis at the adjacent  $\pi$  centre. The positive sign of the pertinent coupling constant can be accounted for by the position of the Me  $\delta$ -protons which are, in general, situated outside the nodal plane of the singly occupied  $\pi$  orbital.

*Alkali-Metal Coupling Constants: Association of Radical Anions with their Counterions.*

The hyperfine splittings from the magnetic nuclei of alkali-metal cations in the ESR spectra of organic radical anions are the most convincing evidence of the association between these anions and their positively charged counterions  $Li^+$ ,  $Na^+$ ,  $K^+$ ,  $Rb^+$ , and  $Cs^+$  [12c]. The pertinent  $^7Li^-$ ,  $^{23}Na^-$ ,  $^{39}K^-$ ,  $^{85,87}Rb^-$ , and  $^{133}Cs^-$ -coupling constants have been determined by ESR [12c][22] [23], NMR [24], and (more recently) ENDOR/general-TRIPLE-resonance spectroscopy [10c] [25]. In the few cases studied by the NMR method, absolute signs were allotted to these coupling constants, albeit use of concentrated solutions frequently modified the mode of association relative to that occurring in diluted solutions investigated by ESR/ENDOR technique. Such a reservation is not required for the general-TRIPLE-resonance experiments performed on the ENDOR spectra. Although only relative signs of the coupling constants are obtained by this technique, absolute signs can readily be derived by means of appropriate reference, as has been done in the present paper (see above). The  $|a_{Li}|$ ,  $|a_{Na}|$ ,  $|a_K|$ , and  $|a_{Cs}|$  values observed here are in a ratio of ca. 2:4:1:8 which has also been found in several other studies [22]. This ratio roughly follows the order of the hyperfine parameters calculated for a unit *ns*-spin density at the alkali-metal atom [26] ( $n=2,3,4$ , and

6 for Li, Na, K, and Cs, respectively), thus indicating similar magnitude of the spin populations in the *ns* orbitals of the various counterions. It has been suggested [22] that the sign of the alkali-metal-coupling constants can be deduced from the temperature dependence of its absolute value. The sign is positive (negative), when this value increases (decreases) on warming the solution. According to this criterion, the coupling constants  $a_{\text{Na}}$ ,  $a_{\text{K}}$ , and  $a_{\text{Cs}}$  determined in the present work should be positive, whereas  $a_{\text{Li}}$  is expected to have a negative sign. Such a prediction is in agreement with the results of general-TRIPLE-resonance spectroscopy as far as  $a_{\text{Li}}$  and  $a_{\text{Cs}}$  are concerned (see above). Association of the radical anions with  $\text{Li}^+$  differs in some aspects from that with  $\text{Na}^+$ ,  $\text{K}^+$ , and  $\text{Cs}^+$ . As stated in a preceding section, two  $\text{Li}^+$  counterions are associated with  $\mathbf{1}^-$ – $\mathbf{10}^-$  against a *single one*  $\text{Na}^+$ ,  $\text{K}^+$ , and  $\text{Cs}^+$ . The formation of these ion triples  $\mathbf{R}^-/2\text{Li}^+$ , instead of ion pairs  $\mathbf{R}^-/\text{Na}^+$ ,  $\mathbf{R}^-/\text{K}^+$ , and  $\mathbf{R}^-/\text{Cs}^+$ , can be formulated as



where  $\mathbf{R}^- = \mathbf{1}^-$ – $\mathbf{10}^-$ . The negative sign of  $a_{\text{Li}}$ , which contrasts with the positive one of  $a_{\text{Na}}$ ,  $a_{\text{K}}$ , and  $a_{\text{Cs}}$ , indicates that, despite similar magnitude of the *ns*-spin populations, the mechanism of electron-spin transfer from the radical anion to the counterion is other for  $\mathbf{R}^-/2 \text{Li}^+$  than for  $\mathbf{R}^-/\text{Na}^+$ ,  $\mathbf{R}^-/\text{K}^+$ , and  $\mathbf{R}^-/\text{Cs}^+$ . Possibly, two predominantly covalent N–Li bonds are formed in the  $\pi$  plane of the azo group, as the ‘hard acid’  $\text{Li}^+$  is akin to the ‘hard base’ represented by the lone pairs of the N-atoms. The spin transfer through these bonds to the Li-atoms should occur by polarization, like that onto the H-atoms directly linked to the  $\pi$  centres. On the other hand, in  $\mathbf{R}^-/\text{Na}^+$ ,  $\mathbf{R}^-/\text{K}^+$ , and  $\mathbf{R}^-/\text{Cs}^+$ , the larger alkali-metal cations being ‘softer acids’ prefer to be attached to the ‘softer base’, which is the  $\pi$  system of azo group; in this case, spin transfer to the counterions should take place by delocalization. A striking example for different modes of association of an organic anion with  $\text{Li}^+$  and  $\text{K}^+$  has been reported in 1978 [27].

**Experimental.** – All compounds were synthesized according to procedures described previously: **1** [28], **2** [29], **3** [29][30], **4** [31], **5** [31], **6** [32], **7** [9], **8** [4][33], **9** [34], and **10** [9][35].

The alkali-metal mirrors, used for the reduction of **4**–**10** were generated from K chips and by thermolysis of  $\text{NaN}_3$  (Fluka) or  $\text{CsN}_3$  (Eastman Kodak). The appearance of radical anions associated with  $\text{K}^+$  upon first contact of **4**–**10** with the Na mirror was due to a  $\text{KN}_3$  impurity present in  $\text{NaN}_3$ . The K content became larger on thermolysis and sublimation, due to the greater volatility of K as compared to Na, and reaction of **4**–**10** with K was favoured, because of the higher reducing power of K relative to Na.

Cyclic voltammograms were recorded on a Metrohm Polarecord E506 with a VA Scanner 612/VA Stand 663. ESR spectra were taken on a Varian-E9 instrument, while a Bruker-ESP-300 system served for ENDOR and TRIPLE-resonance studies.

**Appendix.** – The effect of the  $^{14}\text{N}$ -hyperfine anisotropy on the line-widths ( $lw$ ) in the ESR spectra of  $\mathbf{1}^-$ – $\mathbf{10}^-$  can be expressed as [12][13]

$$lw = A + BM_1 + CM_1^2$$

where A, B, and C are empirical parameters, and  $M_1 = +2, +1, 0, -1, -2$  is the  $^{14}\text{N}$ -spin quantum number which decreases with increasing magnetic field. The  $lw$  values for the individual  $M_1$  components have to be determined experimentally from the heights of the corresponding lines which are inversely proportional to  $(lw)^2$ . As an example, the line-widths thus obtained for  $\mathbf{2}^-$  associated with  $2 \text{Li}^+$  at 203 K amount to 0.214, 0.104, 0.074, 0.124, and 0.254 mT for  $M_1 = +2, +1, 0, -1, \text{ and } -2$ , respectively, involving the parameters  $A = 0.074$ ,  $B = -0.010$ , and  $C = 0.040$  mT. Fig. 7 shows the pertinent ESR spectrum, along with two computer simulations: one of them (1) makes use of a constant line-width, 0.074 mT, characteristic of the central component with  $M_1 = 0$ , while the second (2) employs the five different  $lw$  values given above. Clearly, the second simulation reproduces the

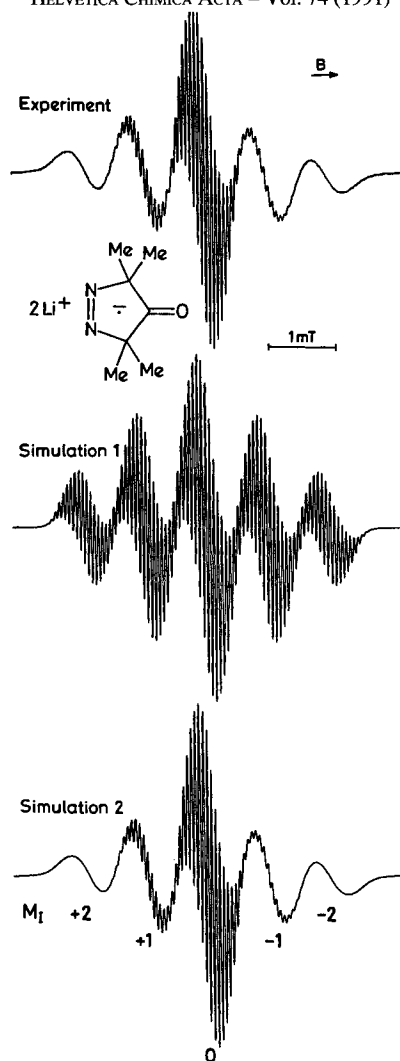


Fig. 7. ESR spectrum of **2** and its simulations. Solvent: DME; counterions as indicated.; temp. 203 K. The simulations made use of the coupling constants given in Table 1. Line-shape: Lorentzian; line-width as indicated in the text: constant for simulation 1 and variable for simulation 2.

experimental spectrum in more details. The computer program for this simulation is presented in [36]. Experimental difficulties in determining the  $lw$  values emerge, when the  $a_N$  is considerably smaller than the sum of the remaining coupling constants, so that the individual  $M_I$  components strongly overlap.

We are obliged to Professor *R.J. Bushby*, Leeds, England for kindly providing us with samples of **2** and **3**. Our thanks are also due to Dr. *J. Lopez* (present address: *Ciba-Geigy*, 1723 Marly) and *U. Buser* of the Basel laboratory for synthesizing **1** and **9**, respectively. Dr. *J. Lopez* carried out some preliminary experiments on **1**–**3**. Financial support by the *Schweizerischer Nationalfonds zur Förderung der wissenschaftlichen Forschung* and the *Deutsche Forschungsgemeinschaft* is acknowledged, as well as that of *Ciba-Geigy AG*, *Sandoz AG*, *F. Hoffmann-La Roche AG*, Basel, and the *Fonds der Chemischen Industrie* of Germany.

## REFERENCES

- [1] J. Thiele, *Ber. Dtsch. Chem. Ges.* **1909**, *42*, 2575.
- [2] P. S. Engel, *Chem. Rev.* **1980**, *80*, 99.
- [3] R. Jain, M. B. Sponsler, F. D. Combs, D. A. Dougherty, *J. Am. Chem. Soc.* **1988**, *110*, 1356.
- [4] W. Adam, G. Reinhard, H. Platsch, J. Wirz, *J. Am. Chem. Soc.* **1990**, *112*, 4570, and references therein.
- [5] W. Adam, O. de Lucchi, *Angew. Chem.* **1980**, *92*, 815; *Angew. Chem. Int. Ed.* **1980**, *19*, 762.
- [6] U. Krynitz, F. Gerson, N. Wiberg, M. Weith, *Angew. Chem.* **1969**, *81*, 745; *Angew. Chem. Int. Ed.* **1969**, *8*, 755.
- [7] R. Sustman, R. Sauer, *J. Chem. Soc., Chem. Commun.* **1985**, 1248.
- [8] G. Gescheidt, A. Lamprecht, C. Rüchardt, M. Schmittel, *Helv. Chim. Acta* **1991**, *74*, 2094.
- [9] W. Adam, S. Grabowski, H. Platsch, K. Hannemann, J. Wirz, R. M. Wilson, *J. Am. Chem. Soc.* **1989**, *111*, 751.
- [10] H. Kurreck, B. Kirste, W. Lubitz, 'Electron Nuclear Double Resonance Spectroscopy of Radicals in Solution', VCH Publishers, Weinheim and New York, 1988; a) Chapt. 2; b) Chapt. 4; c) Chapt. 5.
- [11] F. Gerson, X.-Z. Qin, *Helv. Chim. Acta* **1988**, *71*, 1498.
- [12] F. Gerson, 'High-Resolution ESR Spectroscopy', Wiley, New York and Verlag Chemie, Weinheim, 1970; a) Appendix A. 1.3; b) Chapt. 1.5; c) Appendix A. 2.2.
- [13] A. Hudson, G. R. Luckhurst, *Chem. Rev.* **1969**, *69*, 191.
- [14] G. A. Russell, G. W. Holland, K.-Y. Chang, R. G. Keske, J. Mattox, C. S. C. Chung, K. Stanley, K. Schmitt, R. Blankespoor, Y. Kosugi, *J. Am. Chem. Soc.* **1974**, *96*, 7237.
- [15] F. Gerson, G. Gescheidt, S. F. Nelsen, L. A. Paquette, M. K. Teasley, L. Waykole, *J. Am. Chem. Soc.* **1989**, *111*, 5518.
- [16] J. A. Pople, D. L. Beveridge, 'Approximate Molecular Orbital Theory', McGraw-Hill, New York, 1970.
- [17] M. J. S. Dewar, W. J. Thiel, *J. Am. Chem. Soc.* **1977**, *99*, 4899, 4907.
- [18] U. Buser, C. H. Ess, F. Gerson, *Magn. Reson. Chem.* **1991**, *29*, 721.
- [19] H. Troxler, Diplomarbeit, Universität Basel, 1991.
- [20] C. Heller, H. M. McConnell, *J. Chem. Phys.* **1960**, *32*, 1535; A. Horsfield, J. R. Morton, D. H. Whiffen, *Mol. Phys.* **1961**, *4*, 425.
- [21] R. Hoffmann, A. Imamura, W. J. Hehre, *J. Am. Chem. Soc.* **1968**, *90*, 1499; R. Hoffmann, *Acc. Chem. Res.* **1971**, *4*, 1.
- [22] J. H. Sharp, M. C. R. Symons, in 'Ions and Ion Pairs in Organic Reactions', Ed. M. Szwarc, Wiley-Interscience, New York, 1972; Vol. I, Chapt. 5.
- [23] W. Huber, *Helv. Chim. Acta* **1985**, *68*, 1140.
- [24] G. W. Canters, E. de Boer, B. M. P. Hendriks, H. van Willigen, *Chem. Phys. Lett.* **1968**, *1*, 627; G. W. Canters, E. de Boer, *Mol. Phys.* **1973**, *26*, 1185.
- [25] W. Lubitz, E. Biehl, K. Möbius, *J. Magn. Reson.* **1977**, *27*, 411; W. Lubitz, M. Plato, K. Möbius, R. Biehl, *J. Phys. Chem.* **1979**, *83*, 3402.
- [26] J. R. Morton, K. F. Preston, *J. Magn. Reson.* **1978**, *30*, 577.
- [27] G. Boche, F. Heidenhain, *Angew. Chem.* **1978**, *90*, 290; *Angew. Chem. Int. Ed. Engl.* **1978**, *17*, 283.
- [28] R. J. Crawford, A. Mishra, R. J. Dummell, *J. Am. Chem. Soc.* **1966**, *88*, 3959.
- [29] R. J. Bushby, M. D. Pollard, *J. Chem. Soc. Perkin Trans. 1* **1979**, 2401.
- [30] R. J. Bushby, W. S. McDonald, M. D. Pollard, *Tetrahedron Lett.* **1978**, *19*, 3851.
- [31] R. C. Elder, A. B. Packard, J. W. Rekers, R. M. Wilson, *J. Am. Chem. Soc.* **1980**, *102*, 1633.
- [32] S. L. Buchwalter, G. L. Closs, *J. Am. Chem. Soc.* **1979**, *101*, 4688.
- [33] F. D. Combs, D. A. Dougherty, *Tetrahedron Lett.* **1988**, *29*, 3753; W. Adam, H. Platsch, G. Reinhard, J. Wirz, *J. Am. Chem. Soc.* **1990**, *112*, 4570.
- [34] P. G. Gassmann, K. T. Mansfield, in 'Organic Synthesis', Collective Volume V, Wiley, New York 1973; p. 96 f.
- [35] P. S. Engel, R. T. Grow, D. W. Horsey, D. E. Keys, C. J. Nalepa, *J. Am. Chem. Soc.* **1983**, *105*, 7102.
- [36] C. H. Ess, Dissertation, Universität Basel, 1991.